AEDC-TR-65-62

LIFT, DRAG, AND STATIC STABILITY OF A BLUNT CONICAL MODEL IN HYPERSONIC RAREFIED FLOW

David E. Boylan
ARO, Inc.

March 1965

VON KÁRMÁN GAS DYNAMICS FACILITY
ARNOLD ENGINEERING DEVELOPMENT CENTER
AIR FORCE SYSTEMS COMMAND
ARNOLD AIR FORCE STATION, TENNESSEE

NOTICES

When U. S. Government drawings specifications, or other data are used for any purpose other than a definitely related Government procurement operation, the Government thereby incurs no responsibility nor any obligation whatsoever, and the fact that the Government may have formulated, furnished, or in any way supplied the said drawings, specifications, or other data, is not to be regarded by implication or otherwise, or in any manner licensing the holder or any other person or corporation, or conveying any rights or permission to manufacture, use, or sell any patented invention that may in any way be related thereto.

Qualified users may obtain copies of this report from the Defense Documentation Center.

References to named commercial products in this report are not to be considered in any sense as an endorsement of the product by the United States Air Force or the Government.

LIFT, DRAG, AND STATIC STABILITY OF A BLUNT CONICAL MODEL IN HYPERSONIC RAREFIED FLOW

David E. Boylan
ARO, Inc.

FOREWORD

The research reported herein was sponsored by the Arnold Engineering Development Center (AEDC), Air Force Systems Command (AFSC) under Program Element 62405334, Project 8953. The results of research presented were obtained by ARO, Inc. (a subsidiary of Sverdrup and Parcel, Inc.) contract operator of the Arnold Engineering Development Center (AEDC), AFSC, Arnold Air Force Station, Tennessee, under Contract AF 40(600)-1000. The research was conducted from June 20 to July 15, 1964 under ARO Project VL2407, and the report was submitted by the author on February 23, 1965.

The author acknowledges the contribution of G. D. Arney, Jr. and W. T. Harter, whose work in the design and development of the three-component, low-load balance made these measurements possible.

This technical report has been reviewed and is approved.

Larry R. Walter
1st Lt, USAF
Gas Dynamics Division
DCS/Research

Donald R. Eastman, Jr.
DCS/Research

ABSTRACT

This is a report of results and analysis of measurements of forces on spherically capped cones of 10-deg half-angle, with and without conical afterbodies. These data were obtained during the course of an evaluation of a new three-component balance for use in a low-density, hypersonic wind tunnel. Comparisons are made with modified Newtonian and free-molecule theories. Measurements were made in nitrogen gas at a nominal Mach number of 9.8 and unit Reynolds number of 760 in.$^{-1}$. The suitability of the low-load, three-component balance for measuring aerodynamic forces in low-density flows is demonstrated.

CONTENTS

ILLUSTRATIONS

TABLE

NOMENCLATURE

A_1	Moment arm between moment reference point and L_1 vector
A_2	Moment arm between moment reference point and L_2 vector
A_3	Moment arm between moment reference point and drag force vector
C_A	Axial-force coefficient
C_D	Drag-force coefficient
C_L	Lift-force coefficient
C_M	Static pitching-moment coefficient
C_N	Normal-force coefficient
C_∞	Chapman-Rubesin constant $(\mu_w T_\infty)/\mu_\infty T_w)$
D	Drag force (total of two drag components)
d	Model maximum diameter
L	Model characteristic length
L_1	Lift force (component No. 1)
L_2	Lift force (component No. 2)
M	Mach number
M_p	Static aerodynamic moment about moment reference point
$\dot{m}$	Nozzle mass flow rate
p_o	Reservoir total pressure
p_o'	Stagnation pressure behind a normal shock
q_∞	Free-stream dynamic pressure
Re_o	Unit Reynolds number based on μ_o and conditions behind normal shock - $\rho_2 U_2/\mu_o$
Re_∞	Free-stream Reynolds number

S	Model maximum cross-sectional area
S_∞	Free-stream molecular speed ratio, $U_\infty \left(2RT_\infty\right)^{-1/2}$
T_O	Reservoir temperature
T_W	Wall temperature
T_∞	Free-stream static temperature
U_∞	Free-stream velocity
$\overline{V}_\infty$	Viscous interaction parameter $M_\infty \left(C_\infty / Re_{\infty_L}\right)^{1/2}$
α	Angle of attack
γ	Ratio of specific heats
μ	Coefficient of viscosity

SUBSCRIPTS

2	Conditions behind a normal shock
d	Based on maximum model diameter
L	Based on model characteristic length
o	Reservoir conditions
∞	Free-stream conditions

SECTION I
INTRODUCTION

Multi-component aerodynamic force measurements on typically small scale models in low-density, hypersonic wind tunnels have not been published up to the present time, largely because of the requirement for a balance of sufficient sensitivity and accuracy to measure the small aerodynamic loads. The recent successful development of a three-component balance for use in the low-density, hypersonic wind tunnel (Gas Dynamic Wind Tunnel, Hypersonic (L)) of the von Karman Gas Dynamics Facility (VKF), AEDC, AFSC, has enabled such measurements to be made. This report contains data taken during the balance development period on a small 10-deg half-angle blunt cone which was previously used in studies of aerodynamic drag (Ref. 1). Although it was discovered that failure to achieve the desired accuracy in locating the sting in the models caused excessive uncertainty of moment coefficients, lift and drag were unaffected, and the data clearly seem to warrant publication because of the unique flow conditions.

SECTION II
APPARATUS

2.1 WIND TUNNEL

Tunnel L is a continuous-type, arc-heated, ejector-pumped facility, normally using nitrogen or argon as the test gas and consisting of the following major components in streamwise order:

1. Continuous, water-cooled d-c arc-heater. Thermal Dynamic F-40 or U-50®, both slightly modified, with 40-kw selenium rectifier power supply. Gas is injected without swirl in the F-40 arc heater and with or without swirl in the U-50 unit. Unless otherwise noted, all testing is done without use of swirling gas injection.
2. Cylindrical, water-cooled settling section. Variable size, but normally of 3-in.-diam and 6- to 10-in. length.
3. Axisymmetric, water-cooled aerodynamic nozzle. Variable sizes with 0.10- to 1.20-in.-diam throats and 2.0- to 8.0-in.-diam exits. At this time three contoured nozzles having no flow gradients in the test section are available in addition to older conical nozzles.

4. Cylindrical test-section tank. 48-in. diameter surrounding the test section and containing instrumentation, cooling water connections, and probe carrier.
5. Axisymmetric diffuser. Interchangeable designs for varying test conditions. Convergent entrance, constant-area throat, and divergent exit sections. Water-cooled entrance.
6. Water-cooled heat exchanger.
7. Air ejector of two stages.
8. Connection to the VKF evacuated, 72-ft-diam, spherical vacuum reservoir and its pumping system.

All critical components of the tunnel and related systems are protected by back-side water cooling. The two-stage ejector system is driven by air instead of steam because of the ready availability of high pressure air at the tunnel site. Although the working gas normally is nitrogen or argon, other gases may be used.

2.2 NOZZLE FLOW CONDITIONS

The data were obtained using a semi-contoured axisymmetric nozzle designed for use with nitrogen as the working gas. Since the development of the three-component balance was the primary purpose of this test, the flow conditions were limited to a single condition as follows:

Test Region - at aerodynamic nozzle exit with 2.52-in. extension in place

p_o = 20.0 psia	q_∞ = 5.45 lb/ft^2
$\dot{m}$ = 5.85 lb_m/hr	Re_o/in. = 95
T_o = 2200°K	T_∞ = 113°K
M_∞ = 9.8	S_∞ = 8.2
Re_∞/in. = 760	

This particular flow condition was chosen to duplicate precisely one set of data presented in Ref. 1, thereby obtaining direct comparison of the drag measurements with previous one-component balance data. Using the characteristic length as defined in Fig. 1, the value of the viscous interaction parameter, $\overline{V}_\infty$, is 0.40 for the Type A models and 0.316 for the Type B models.

Transverse impact pressure measurements taken at the test position are shown in Fig. 2 and indicate a usable core size of 0.8 in. The influence of axial-flow gradients in the test region is negligible because of the small model length.

2.3 MODELS

The basic configuration of the models is a 10-deg semi-vertex blunted cone with a modified spherical nose segment. This shape has been proposed for an instrument capsule to be used for planetary atmospheric studies. Two types of models were tested, one with a flat base and one with a 50-deg semi-vertex conical afterbody. The flat-based model is designated Type A, and the model with conical afterbody is designated Type B. The models are shown in Fig. 1 with a tabulation of the angles of attack applicable to each model.

At the time of model construction, a literature survey indicated that in previous tests of these shapes, moment was referenced to a point 42 percent of the base diameter behind the model nose. The models were therefore designed for the sting axis to pass through this point to eliminate drag-force influence on the pitching moment. A later literature search revealed that other data were taken using, as a moment reference, a point on the model centerline at 48.2 percent of the base diameter measured from the model nose. The data in the present report have been based on this latter position which is indicated in Fig. 1. However, a subsequent examination of the models revealed that, because of fabrication errors, the model mounting trunnion was positioned at neither of these stations, and an additional term in the solution for the static pitching moment was necessary to account for the drag influence. This caused much more than ordinary scatter and uncertainty in some of the moment data. Despite this error, the report is published because of widespread interest in data for the conditions simulating very high altitude.

2.4 THREE-COMPONENT FORCE BALANCE

The balance is of the external type and is composed of two drag and two lift links. Pitching moment is intended to be derived from the two lift links. The drag-force component is measured through two restoring links as a matter of convenience, thus allowing determination of an additional moment. However, at this time only pitching moment was determined. All components operate on the nulling principle. The mechanical arrangement of the balance is shown in Fig. 3. A complete description is given in Ref. 2 with a discussion of the balance performance evaluation and accuracy.

The model aerodynamic static pitching moment is resolved from the lift and drag forces and measured moment arm lengths. This is illustrated schematically by the following example:

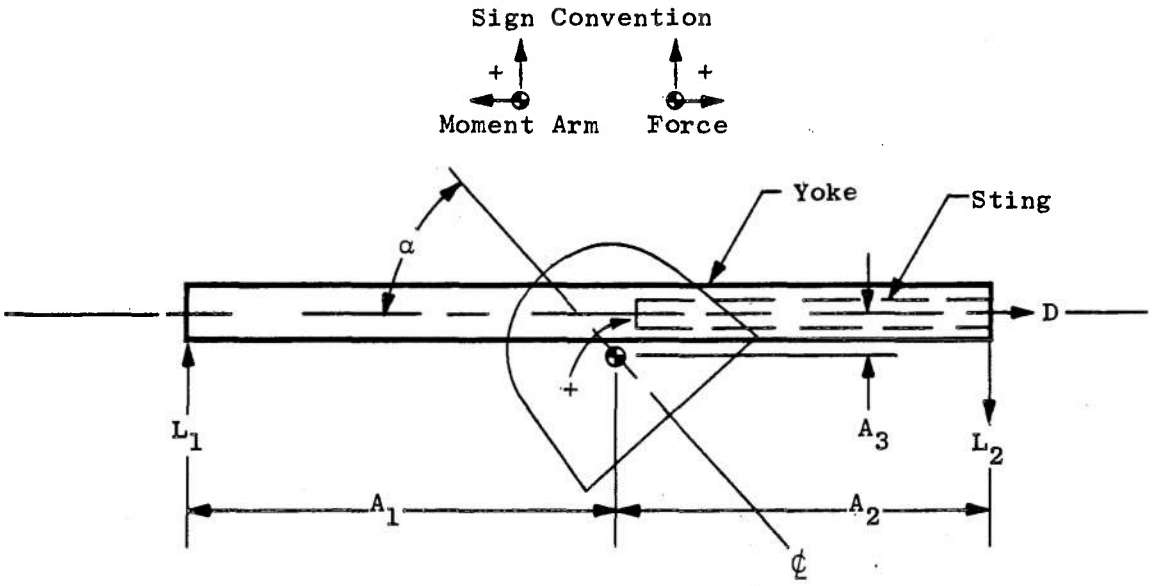

$$M_p = (A_1)(L_1) + (-A_2)(-L_2) + (A_3)(D) \qquad (1)$$

Moment arms A_1 and A_2 are measured using a known reference on the balance sting and the known distance between the two lift components. Moment arm A_3 was determined in part by placing the models on an optical comparator with a dummy sting in place. Figure 4 is a typical result of this investigation. Although several traces were made of each model at random roll positions, the accuracy of determining A_3 was such that a degree of uncertainty was introduced into the solution of static pitching moment.

Aerodynamic forces L_1, L_2, and D are measured as individual lift forces and the sum of the two drag forces, each of which registered one-half of the total drag force.

It is assumed that the sting mount was correctly placed on the model centerline. This was indicated to be essentially correct from the several measurements of moment arm, A_3, which were made on each model and by the fact that each drag component registered one-half the total drag.

SECTION III
EXPERIMENTAL PROCEDURE AND RESULTS

To check for flow angularity, the models were tested both at positive and negative angles of attack, i.e., nose-up and nose-down. Test duration was on the order of 45 sec to prevent excessive heating of the balance and to retain cold-wall model conditions. The wall-to-stagnation temperature ratio was estimated at approximately 0.30.

The aerodynamic forces acting on the model may be calculated from the balance restoring force measurements and expressed in coefficient form from the following relationships for the flow conditions of the present test. Force units are in lb_f and moment units are in in.-lb_f.

$$\left.\begin{aligned} C_M &= M_p/q_\infty\, S d = 269.11\, M_p \\ C_D &= D/q_\infty\, S = 134.55\, D \\ C_L &= (L_1 + L_2)/q_\infty\, S = 134.55\, (L_1 + L_2) \end{aligned}\right\} \qquad (2)$$

The reduced data using Eq. (2) are listed in Table I. Figures 5 through 6 show the variation of C_D and C_L as a function of angle of attack. Since no flow angularity could be detected, data from Table I were plotted with no distinction being made between positive and negative attitudes. Appropriate sign changes were made in plotting the data. Included in Table I are values of the moment arms A_1, A_2, and A_3. The values of A_3 are averages of several measurements. Figure 7 shows the variation of C_M with angle of attack. The estimated degree of reliability is indicated at each angle of attack from an examination of separate data points. Included in Fig. 7 are data of Ref. 3 at $M_\infty = 15$ in helium at a Reynolds number of 2.25×10^6 based on model maximum diameter. The data taken at $\alpha = 140$ and 170 deg with model Type B were lost because a model modification prevented the determination of moment arm, A_3. The modification was made before the discovery that the error in fabrication described earlier made $A_3 \neq 0$.

An estimate of the error from run-to-run repeatability and balance calibration behavior indicates the lift and drag measurements for model Type A are quite good (±5 percent). Therefore, the static pitching-moment error is assumed to be introduced by the error in model fabrication rather than in the force measurements.

The data in Fig. 6b for the Type B model appear to be questionable inasmuch as the lift coefficients do not fall between those predicted by

inviscid Newtonian and free-molecule theory. However, the lift forces of the Type B model at 140 deg $\leq \alpha \leq$ 180 deg are much smaller than the Type A model (Fig. 6a), and the trend of the data agrees quite well with the theoretical calculations. The maximum value of the lift forces shown in Fig. 6b is approximately 1.4×10^{-4} lb_f, which is at the extreme low end of the balance capability. Thus, confidence in these particular data should be restrained. However, it is noteworthy that corresponding normal-force coefficients in Fig. 9b seem quite plausible.

Since prior published data on these models (Refs. 3 through 9) generally are presented in terms of the force coefficients, C_A, C_N, and C_M, the present data were converted to obtain a direct comparison, using the relationships

$$\left.\begin{aligned} C_N &= C_L \cos\alpha + C_D \sin\alpha \\ C_A &= C_D \cos\alpha - C_L \sin\alpha \end{aligned}\right\} \qquad (3)$$

Average values of C_L and C_D at a given angle of attack were used for the calculation, and the results are presented in Figs. 8 through 9. Included are typical data from Ref. 3 at $M_\infty = 15$ in helium at a Reynolds number of 2.25×10^6 based on model maximum diameter.

Theoretical calculations shown in Figs. 5 through 9 are limited to the two extremes of high Reynolds number, non-viscous theory and free-molecular flow theory. The Newtonian-flow theoretical calculations were taken from Ref. 3 and converted to C_L and C_D. It is assumed that the pressure coefficient is zero on all parts of the body not facing the free stream. The data of Ref. 3 shown in Figs. 7, 8, and 9 were taken using helium as the test medium and are compared to the theoretical curve for $\gamma = 1.4$. However, the effect of γ is quite small in the present case, and comparisons between data taken in helium and air in Ref. 3 show little difference.

The free-molecule flow solutions, shown in the figures, were calculated using the method of Sentman (Ref. 10). The speed ratio value of 7.0 used in the calculation is not identical to the actual free-stream value of 8.2 during the present test. This is because the calculation was done for a previous application (Ref. 1). Since the effect of speed ratio (at high values of the speed ratio) is small, the calculation was not repeated. A wall-to-free-stream temperature ratio of 6.0 was estimated, and fully accommodated diffuse reflection was assumed.

Comparison between the data of Tunnel L with modified Newtonian and free-molecule flow theories indicates large departures from Newtonian

theory caused by viscous interaction effects arising because of the high Mach number and very high simulated altitude in this test.

Newtonian theory predicts the behavior of the model quite well when viscous interaction effects may be neglected, as shown by data from tunnels generating high Reynolds numbers. This agreement is true except for model Type A in the range 140 deg $\leq \alpha \leq$ 180 deg angle of attack. Experiments have shown (Fig. 7a) that the model is statically stable about 180 deg rather than unstable as predicted by Newtonian theory. Results from Tunnel L qualitatively agree with these experimental results.

SECTION IV
CONCLUDING DISCUSSION

The primary purpose of obtaining the data presented in this report was to evaluate the performance of the low-load, three-component balance. However, the data are of interest purely from an aerodynamic viewpoint insofar as they represent unique and useful measurements on a vehicle shape of current interest, under flow conditions which essentially simulate flight conditions at high altitude in a Martian atmosphere. Because of the effective freezing of thermochemical fluid processes at low densities, the Earth's atmosphere also was simulated in this test using nitrogen gas.

The lift and drag force data appear to be reliable, following the theoretical trends and indicating the expected departures from inviscid Newtonian theory. The static pitching-moment data must be considered qualitative because of a fabrication error which necessitated the inclusion of the large drag force in resolving the aerodynamic moment. However, the trends of the static pitching-moment data were as expected. The suitability of the low-load, three-component balance for aerodynamic force tests in low-density flows is demonstrated.

REFERENCES

1. Boylan, David E. and Sims, William H. "Experimental Determination of Aerodynamic Drag on a Blunted 10-deg Cone at Angles of Attack in Hypersonic, Rarefied Flow." AEDC-TDR-64-60 (AD 435860), April 1964.

2. Arney, G. D. and Harter, Wade T. "A Low-Load Three-Component Force Balance for Measurements in a Low-Density Wind Tunnel." Proceedings of the 1st International Congress on Instrumentation in Aerospace Simulation Facilities, Paris 1964.

3. Fohrman, Melvin J. "Static Aerodynamic Characteristics of a Short Blunt 10° Semivertex Angle Cone at a Mach Number of 15 in Helium." NASA TN D-1648, February 1963.

4. Treon, Stuart L. "Static Aerodynamic Characteristics of Short Blunt Cones with Various Nose and Base Cone Angles at Mach Numbers of 0.6 to 5.5 and Angles of Attack to 180°." NASA TN D-1327, May 1962.

5. Intrieri, Peter F. "Free-Flight Measurements of the Static and Dynamic Stability and Drag of a 10° Blunted Cone at Mach Numbers 3.5 and 8.5." NASA TN D-1299, May 1962.

6. Wehrend, William R., Jr. "Wind-Tunnel Investigation of the Static and Dynamic Stability Characteristics of a 10° Semivertex Angle Blunted Cone." NASA TN D-1202, January 1962.

7. Compton, Dale L. "Free-Flight Measurements of Drag and Static Stability for a Blunt-Nosed 10° Half-Angle Cone at Mach Number 15." NASA TM X-507, April 1961.

8. Peterson, Victor L. "Motions of a Short 10° Blunted Cone Entering a Martian Atmosphere at Arbitrary Angles of Attack and Arbitrary Pitching Rates." NASA TN D-1326, May 1962.

9. Jaffe, P. "Optimizing the Aft Configuration of a Passive-Entry Capsule." Journal of the Aerospace Sciences, Vol. 29, No. 11, November 1962, pp. 1388-1389.

10. Sentman, Lee H. "Free Molecule Flow Theory and Its Application to the Determination of Aerodynamic Forces." Lockheed Missiles and Space Division, Lockheed Aircraft Corporation, LMSC-448514, October 1961.

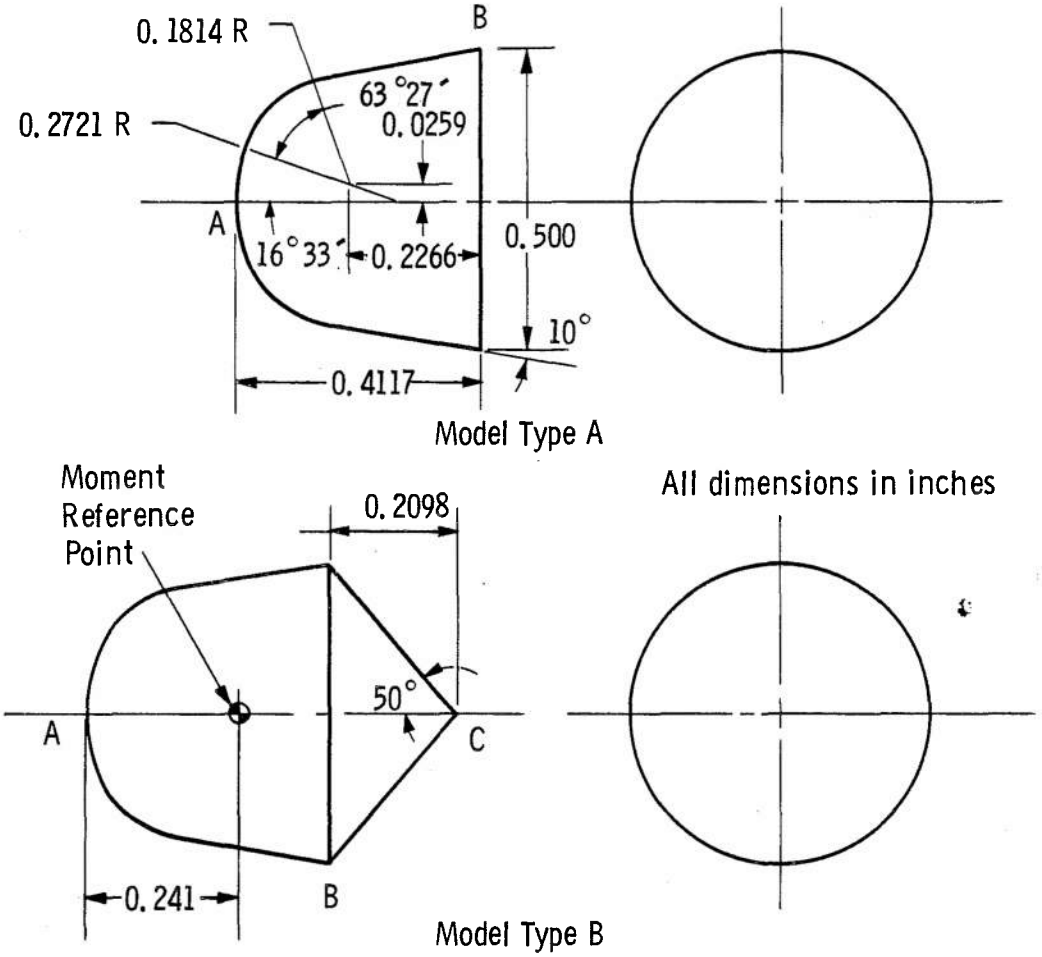

(Type A with Conical Afterbody)

Number	Type	Angle of Attack	L, in.*
1	A	0	0.542
2	A	10°	0.542
3	A	20°	0.542
4	A	31°26′	0.542
5	A	40°	0.542
6	A	170°32′ and 140°55′	0.542
7	A	160° and 150°	0.542
8	B	167°57′ and 140°23′	0.869
9	B	159°50′ and 150°13′	0.869

*The characteristic length (L) is defined as the distance AB in the sketch of the Type A model and the distance ABC in the sketch of the Type B model.

Fig. 1 Model Dimensions and Angles of Attack

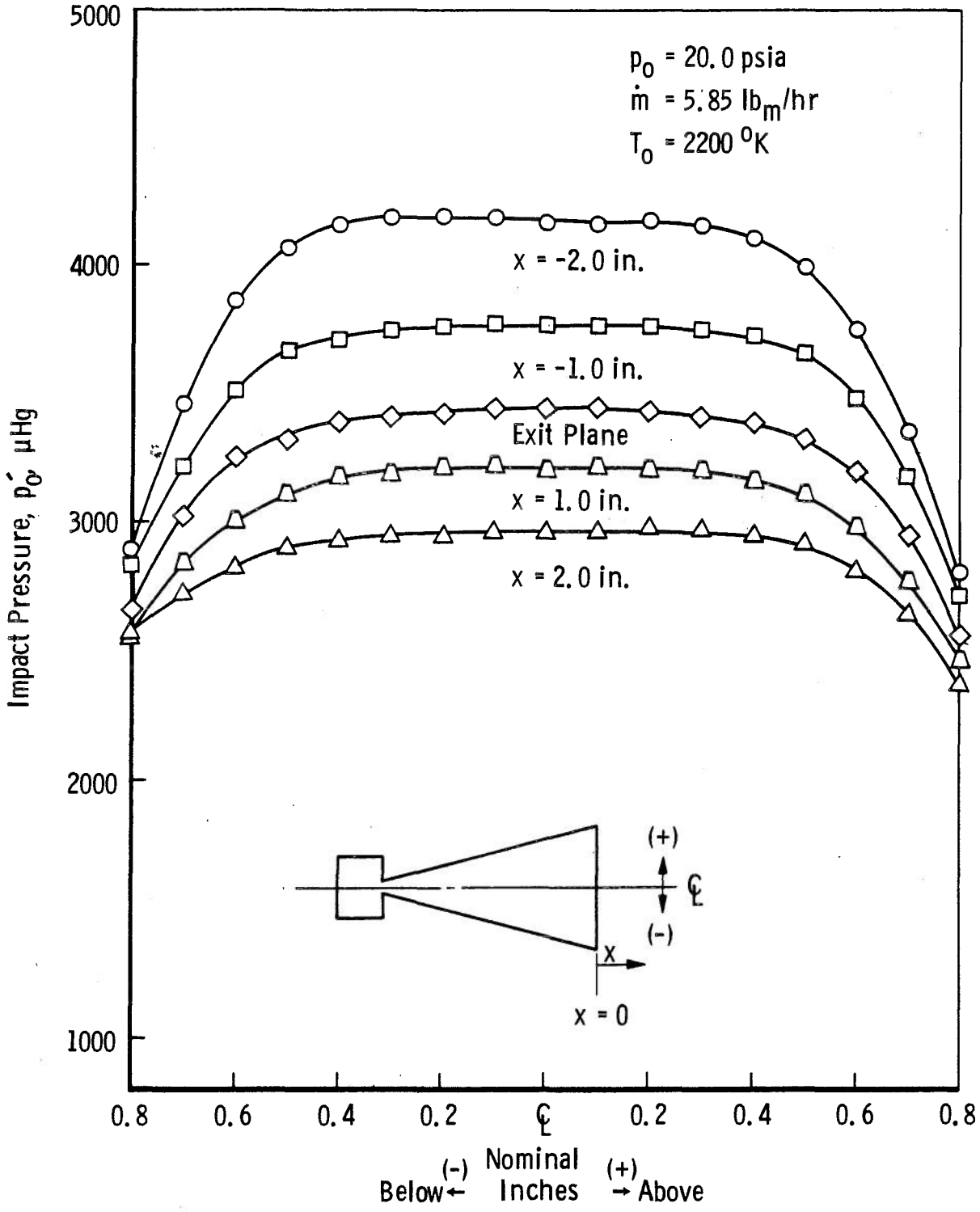

Fig. 2 Nozzle Flow Survey

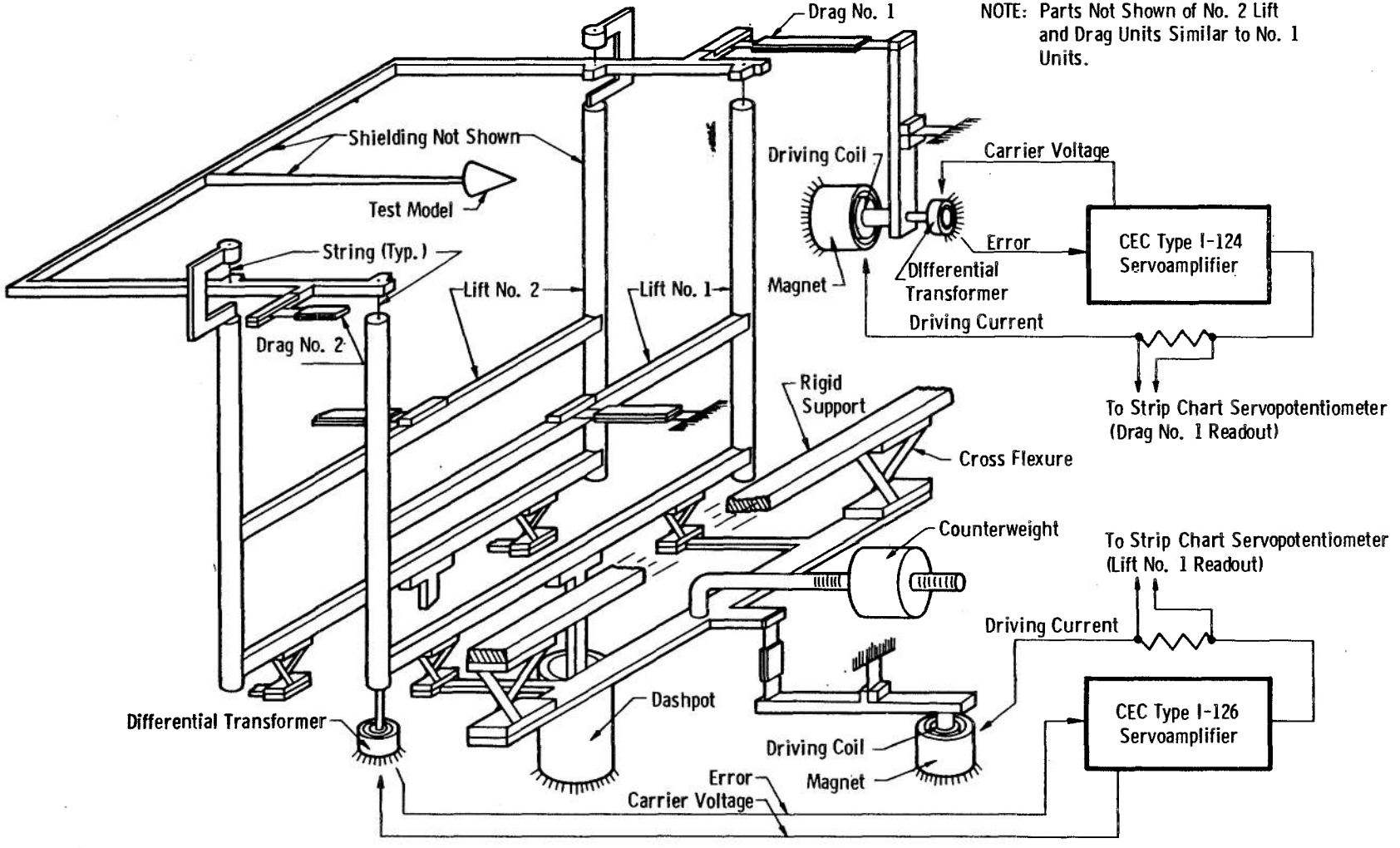

Fig. 3 Balance Schematic (Ref. 2)

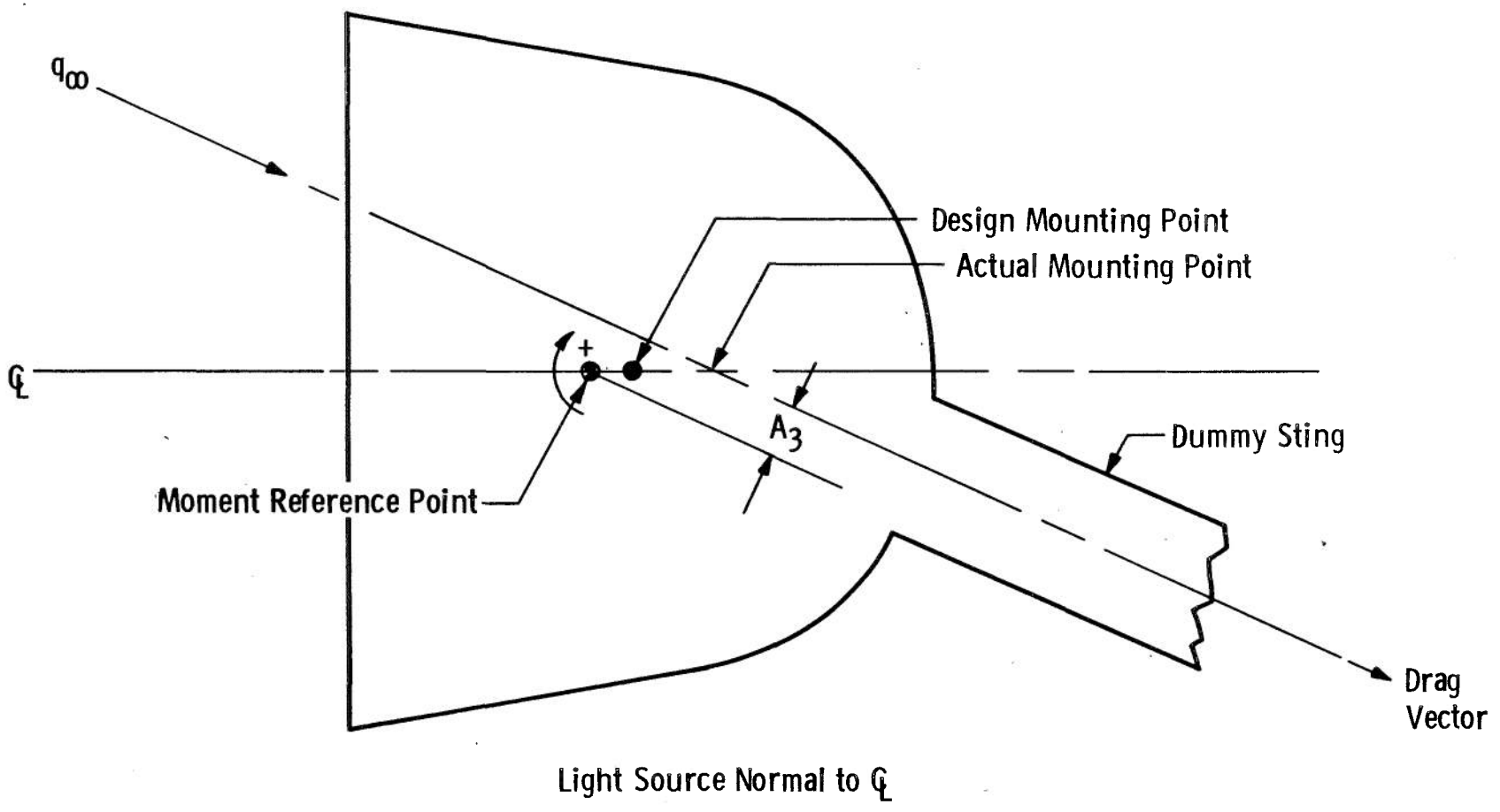

Fig. 4 Moment Arm A_3 Determination

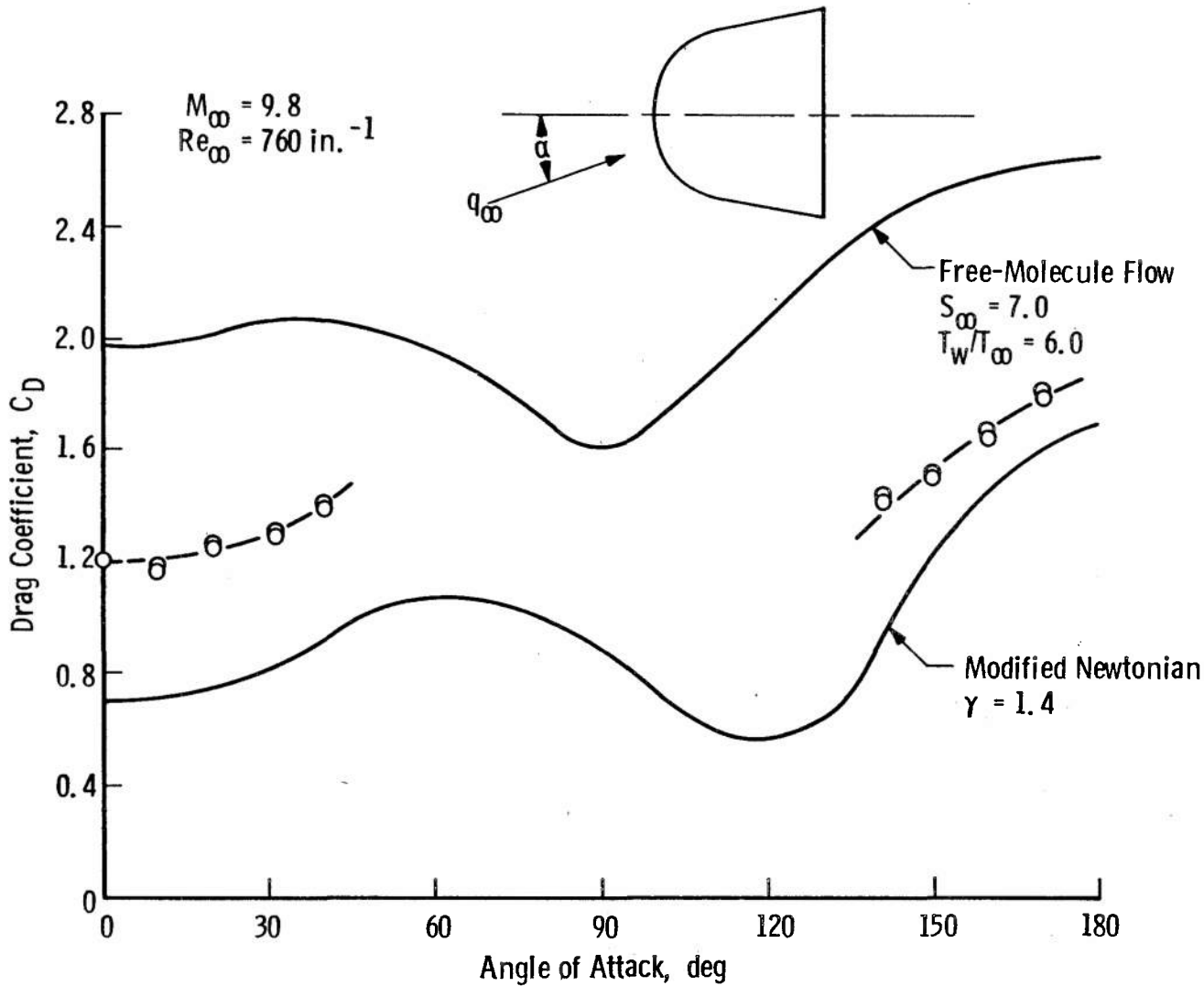

a. Model Type A

Fig. 5 Measured Aerodynamic Drag Coefficient

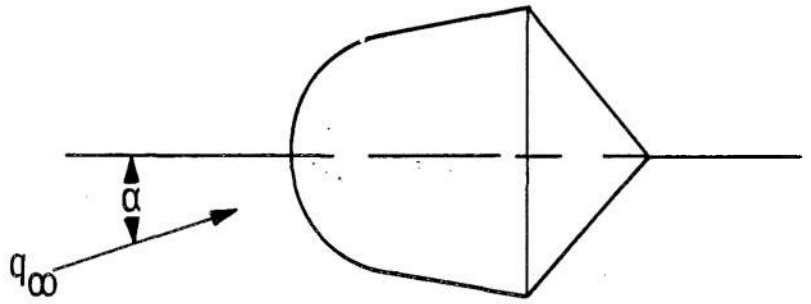

$M_\infty = 9.8$
$Re_\infty = 760$ in.$^{-1}$

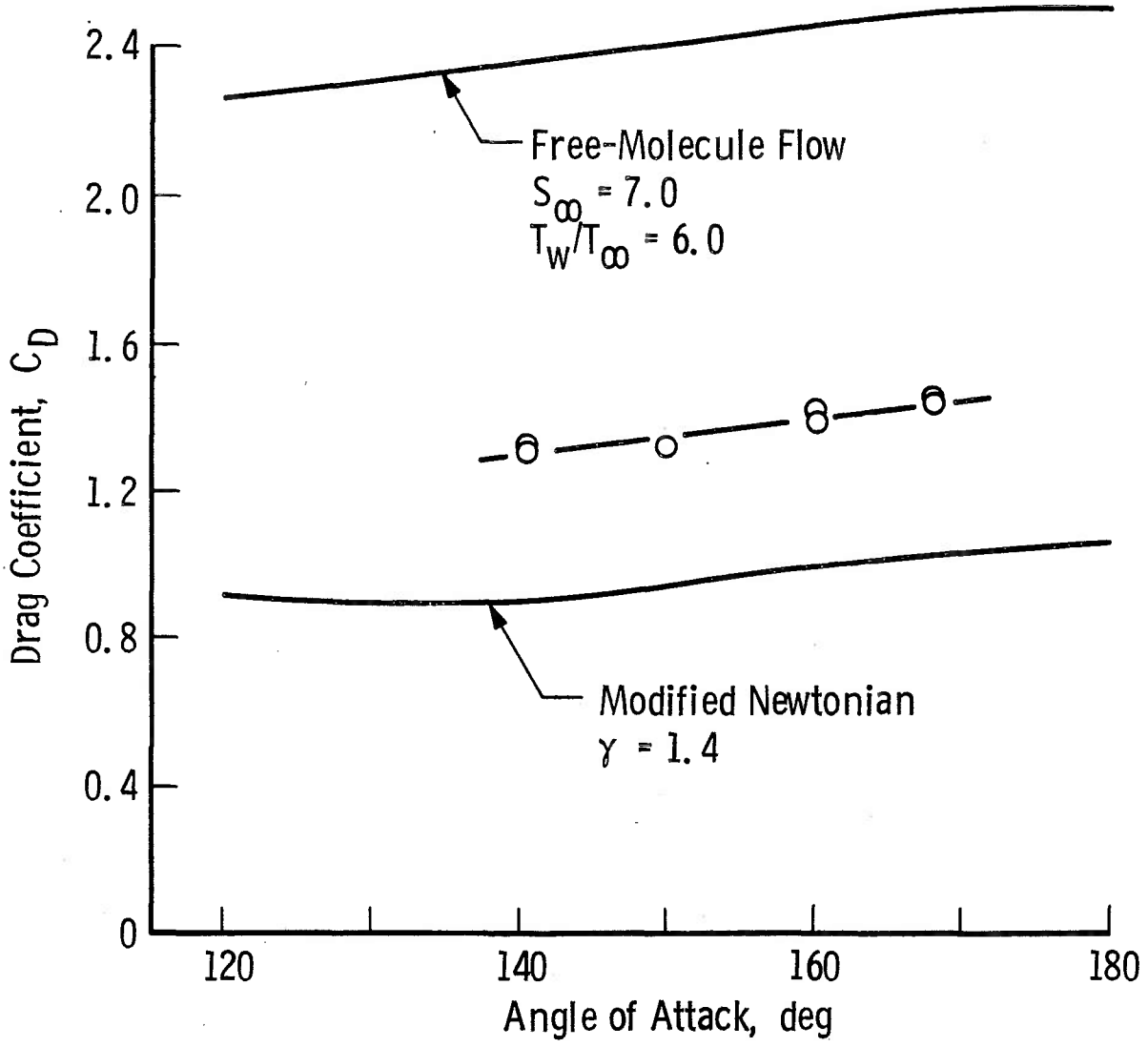

b. Model Type B

Fig. 5 Concluded

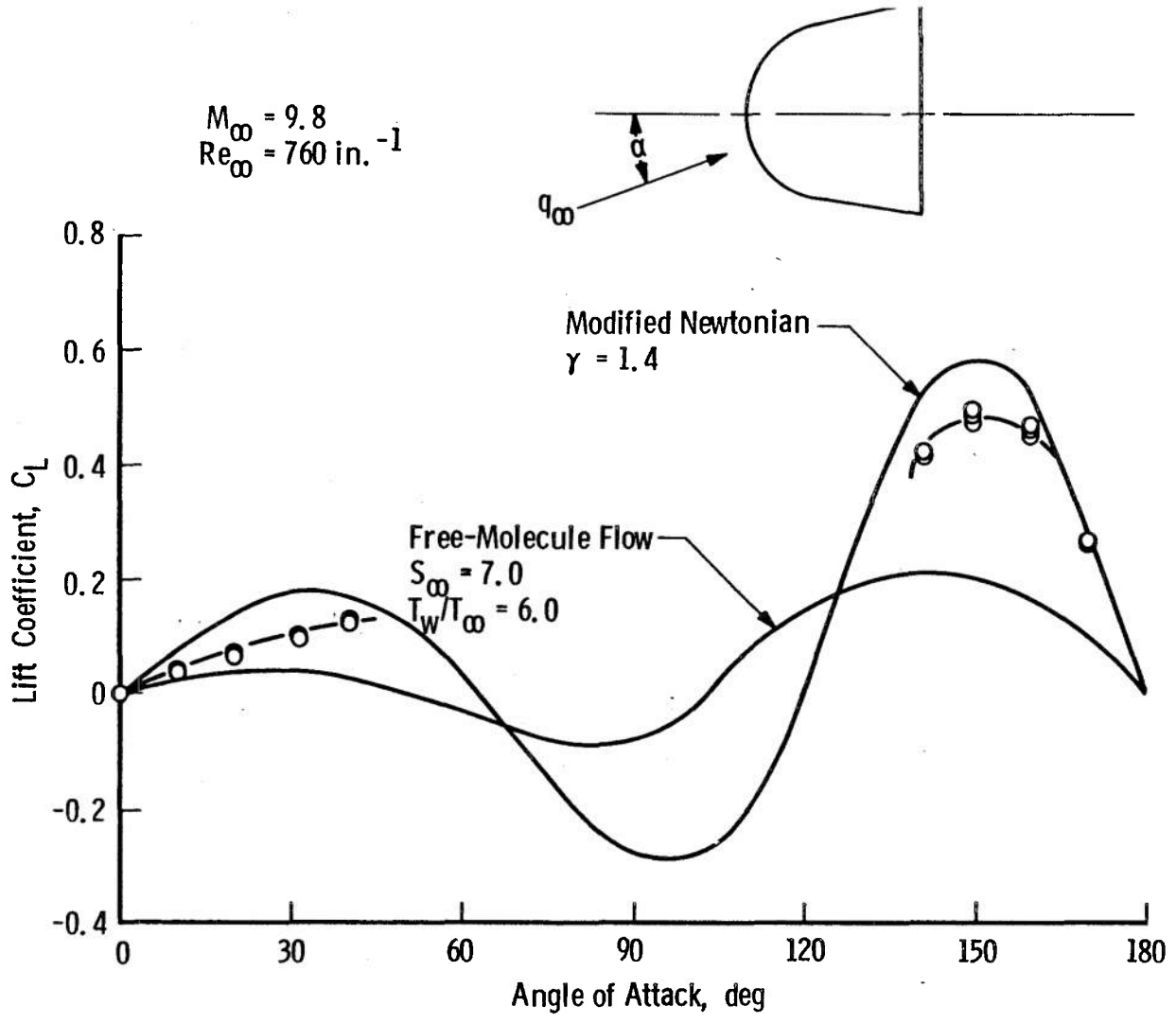

a. Model Type A

Fig. 6 Measured Aerodynamic Lift Coefficient

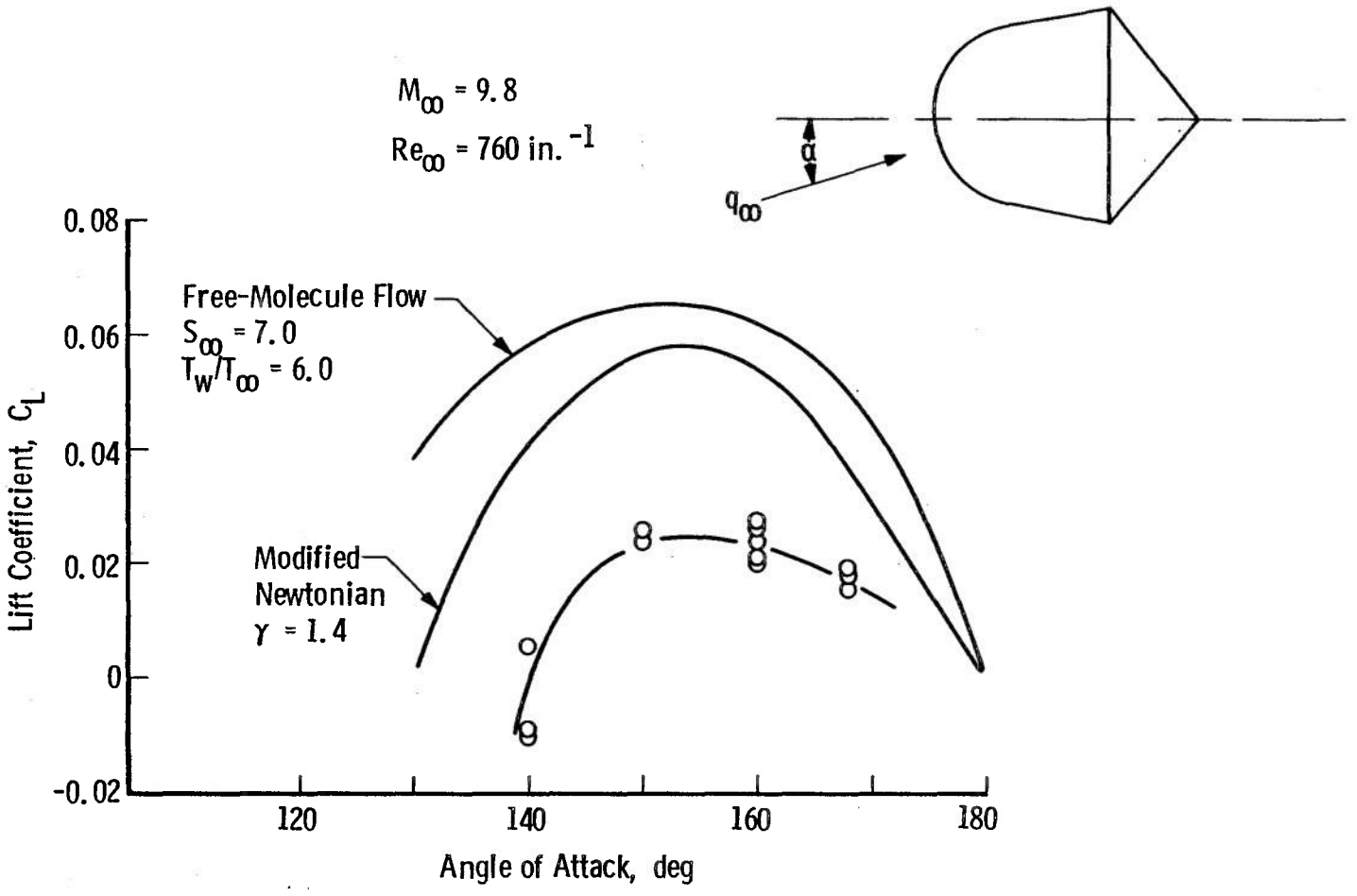

b. Model Type B

Fig. 6 Concluded

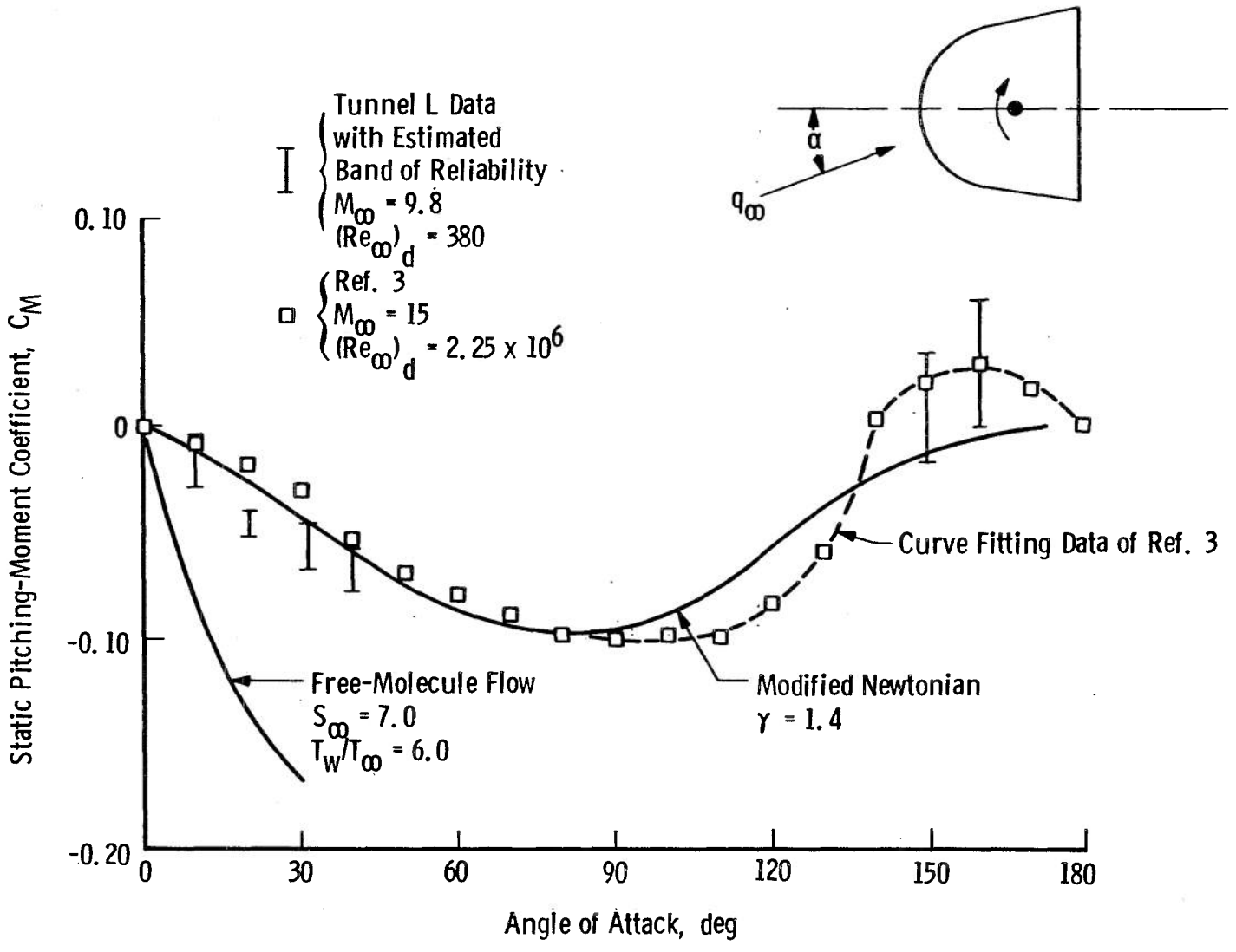

a. Model Type A

Fig. 7 Measured Static Pitching-Moment Coefficient

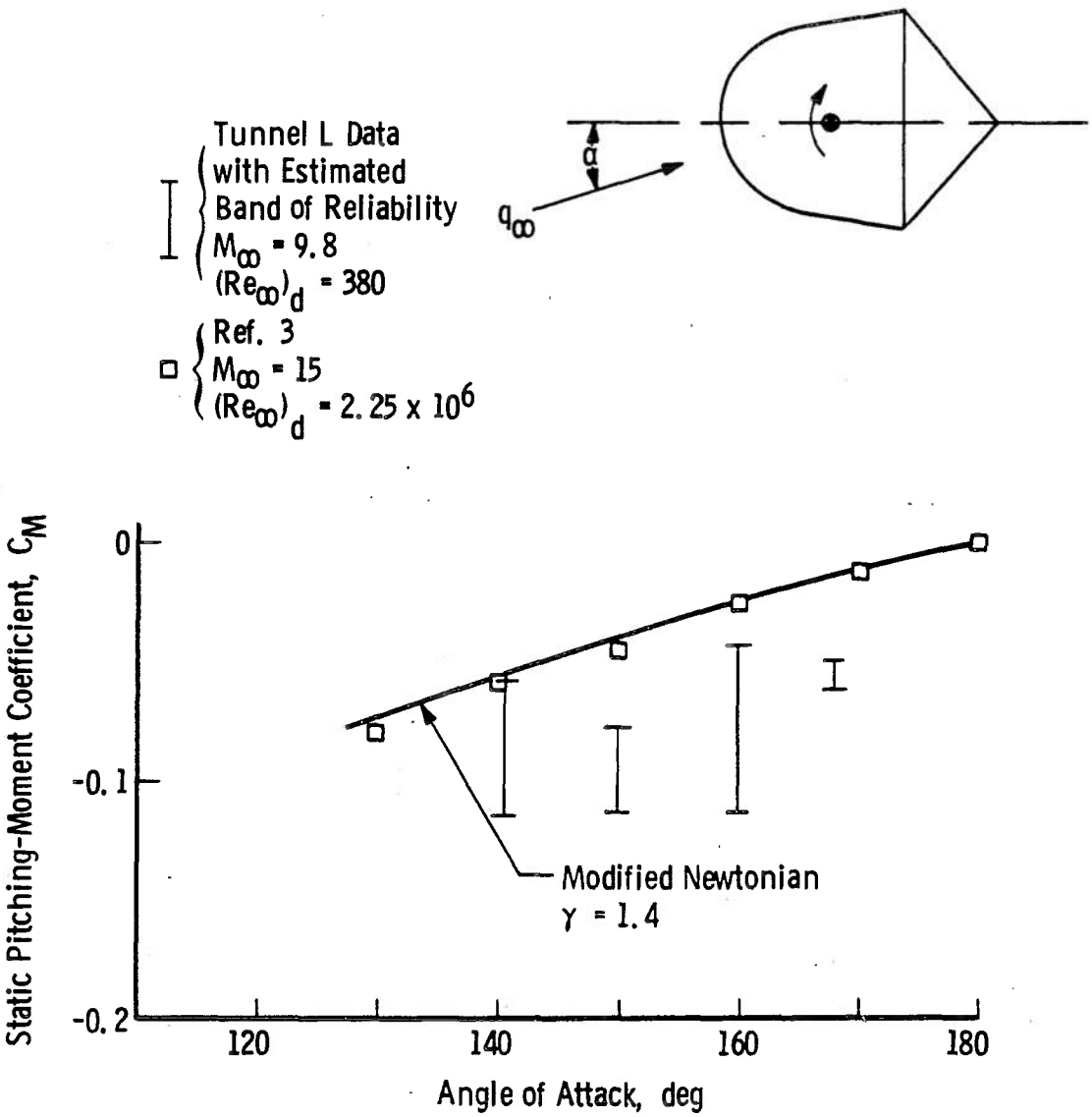

b. Model Type B

Fig. 7 Concluded

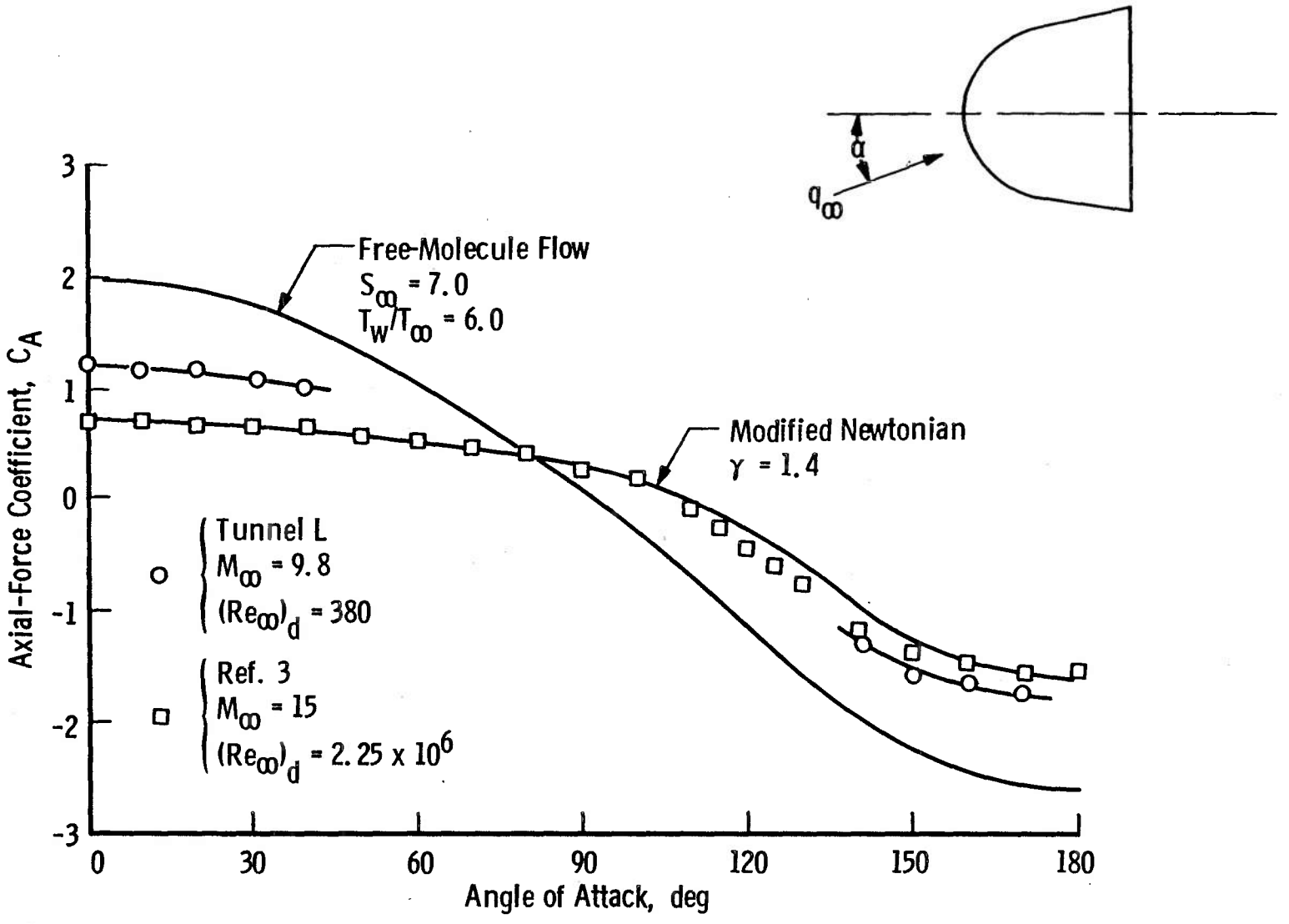

a. Model Type A

Fig. 8 Axial-Force Coefficient Calculated from Average Lift and Drag Measurements

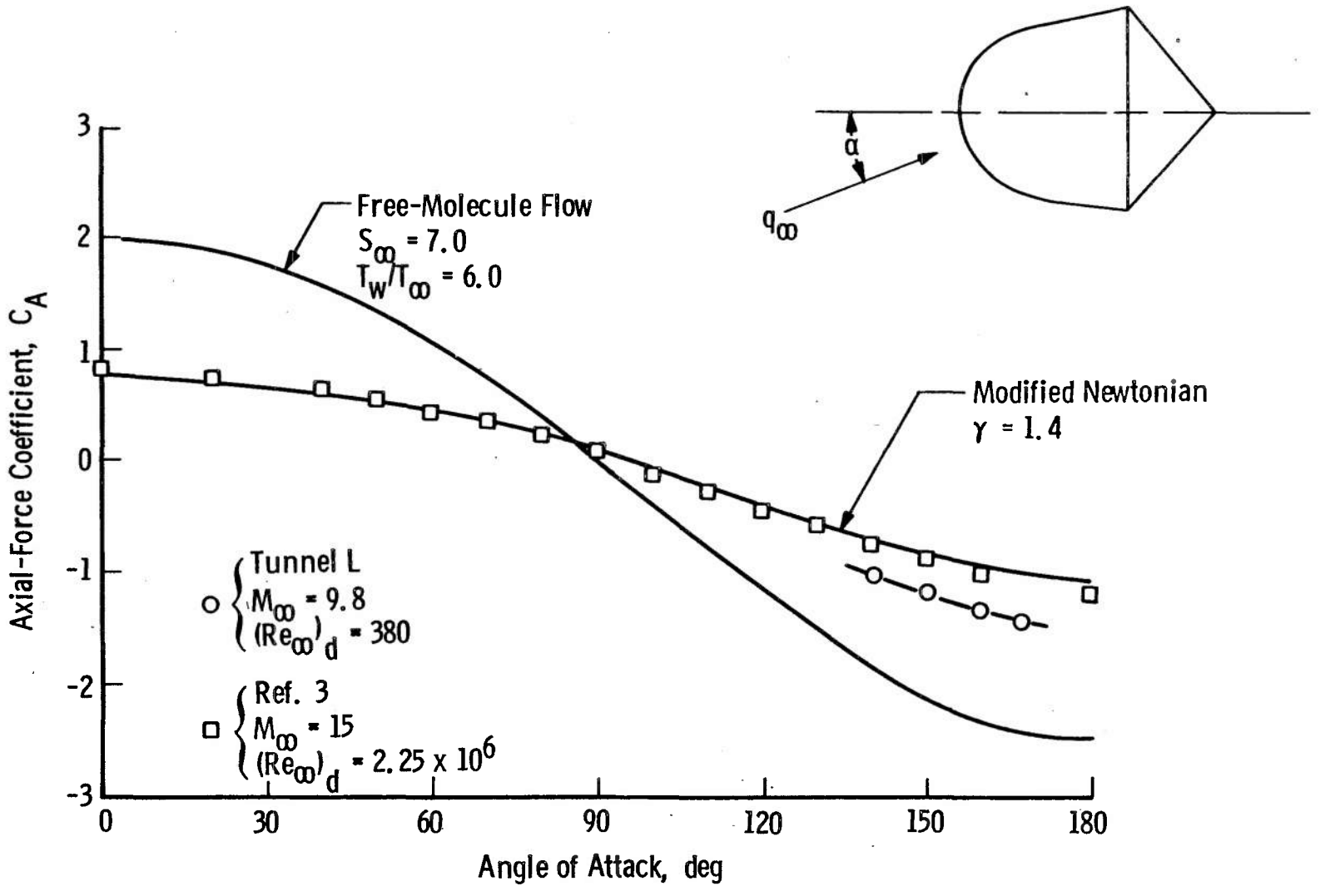

b. Model Type B

Fig. 8 Concluded

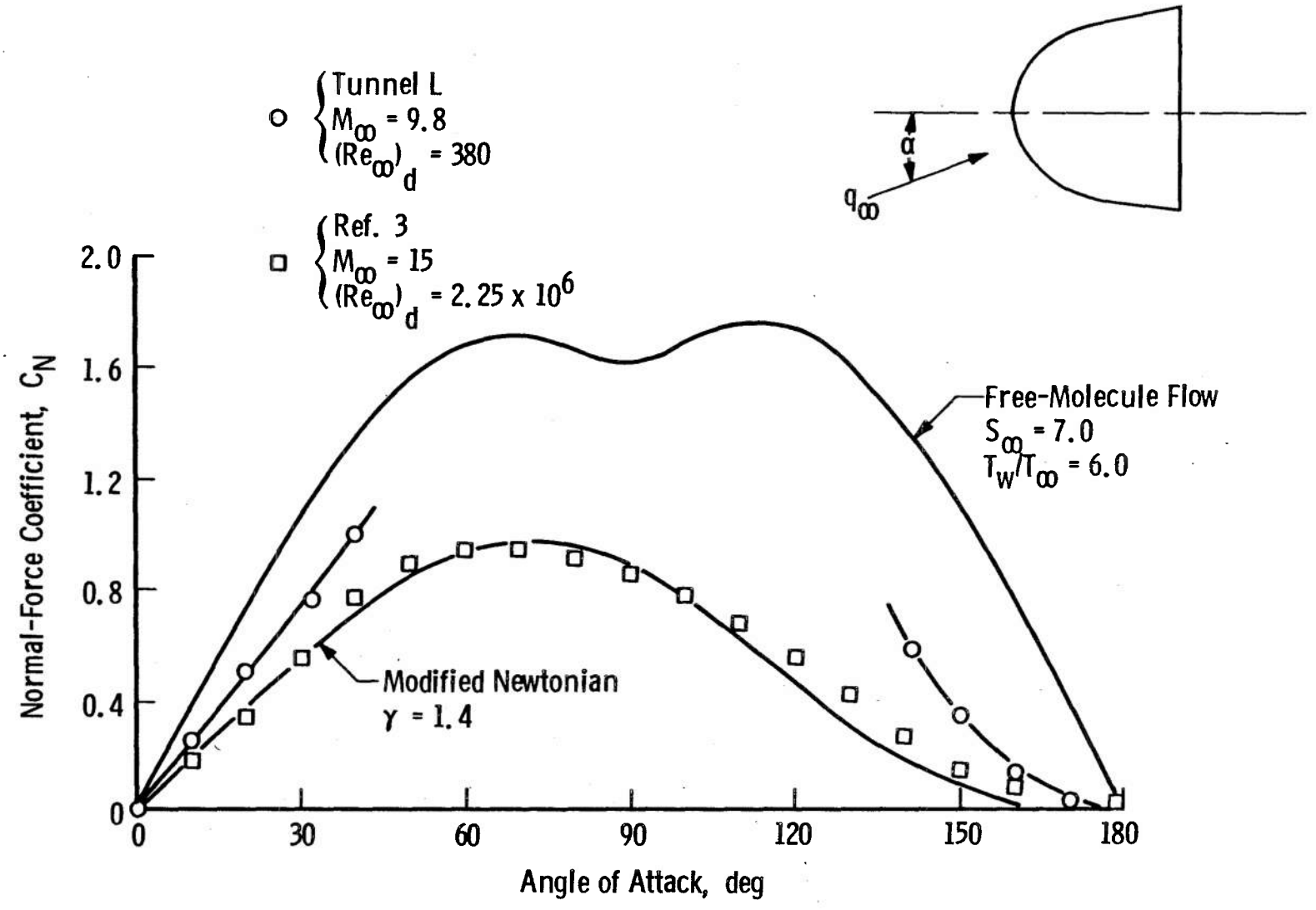

a. Model Type A

Fig. 9 Normal-Force Coefficients Calculated from Average Lift and Drag Measurements

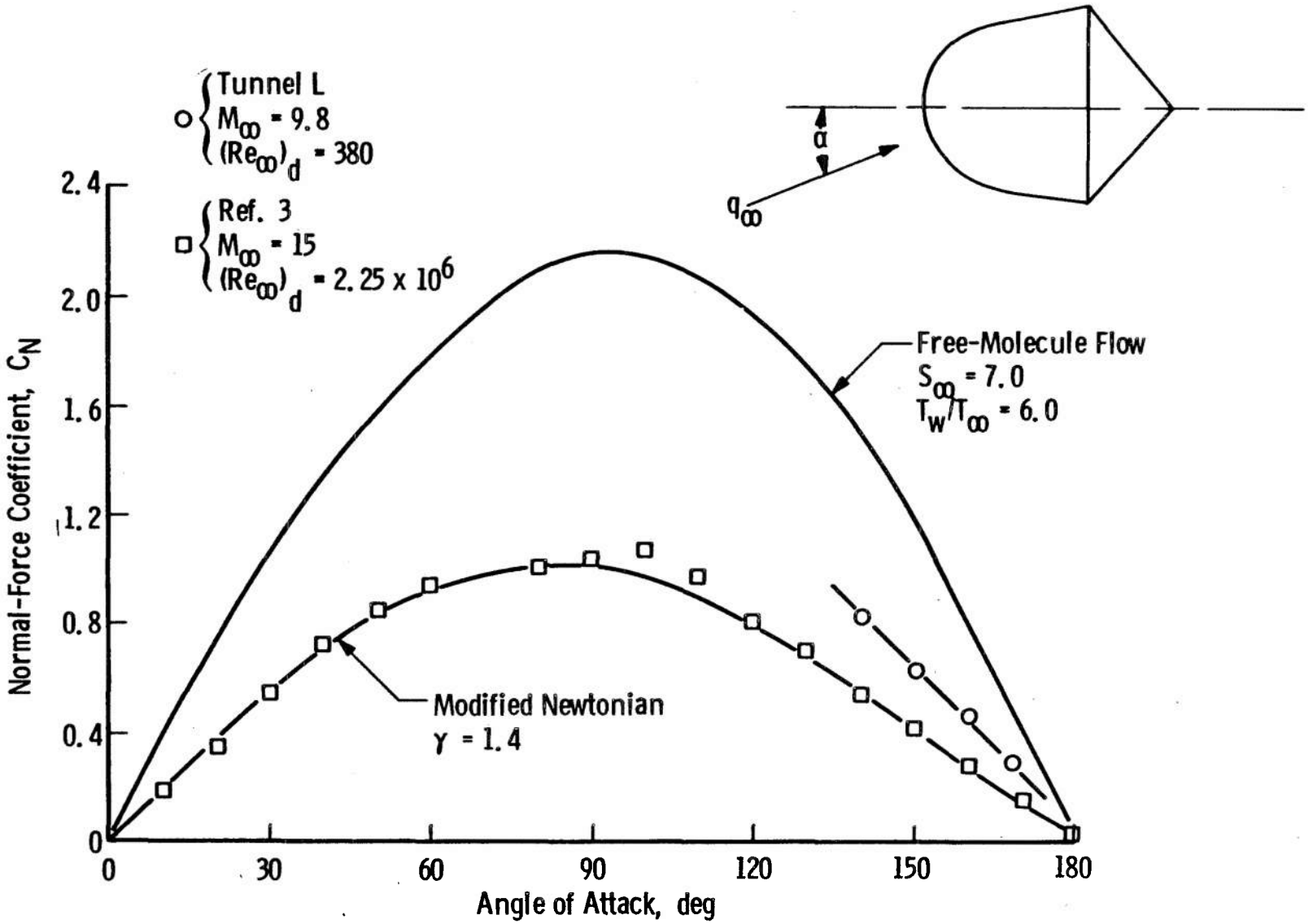

b. Model Type B

Fig. 9 Concluded

TABLE I
TEST DATA

Run	Model	α, deg	A_1, in.	A_2, in.	A_3, in.	L_1, lb_f	L_2, lb_f	D, lb_f	C_L	C_D	C_M
39	1	0	1.214	-7.86^{-1}	0	0	0	8.928^{-3}	-0	1.20	0
40	2	-10	1.214	-7.86^{-1}	-4.20^{-3}	-5.05^{-5}	-20.75^{-5}	8.581^{-3}	-3.47^{-2}	1.16	1.77^{-2}
41	2	10	1.214	-7.86^{-1}	4.20^{-3}	6.07^{-5}	20.75^{-5}	8.730^{-3}	3.61^{-2}	1.18	-1.42^{-2}
42	3	-20	1.206	-7.94^{-1}	-2.35^{-3}	-9.44^{-5}	-38.85^{-5}	9.226^{-3}	-6.50^{-2}	1.24	4.85^{-2}
43	3	20	1.206	-7.94^{-1}	2.35^{-3}	9.77^{-5}	38.60^{-5}	9.374^{-3}	6.51^{-2}	1.26	-4.48^{-2}
45	4	-31°26'	1.190	-8.10^{-1}	-1.04^{-2}	-11.46^{-5}	-56.70^{-5}	9.572^{-3}	-9.17^{-2}	1.29	6.01^{-2}
46	4	31°26'	1.190	-8.10^{-1}	1.04^{-2}	12.80^{-5}	57.30^{-5}	9.721^{-3}	9.43^{-2}	1.31	-5.67^{-2}
47	5	-40	1.165	-8.35^{-1}	-1.06^{-2}	-20.90^{-5}	-72.50^{-5}	10.267^{-3}	-12.57^{-2}	1.38	6.81^{-2}
48	5	40	1.165	-8.35^{-1}	1.06^{-2}	20.55^{-5}	73.90^{-5}	10.465^{-3}	12.71^{-2}	1.41	-7.18^{-2}
76	7	200	1.142	-8.58^{-1}	-3.51^{-2}	-129.4^{-5}	-202.2^{-5}	12.35^{-3}	-4.46^{-1}	1.66	-4.84^{-2}
		200	1.142	-8.58^{-1}	-3.51^{-2}	-129.7^{-5}	-201.2^{-5}	12.35^{-3}	-4.45^{-1}		-5.07^{-2}
		200	1.142	-8.58^{-1}	-3.51^{-2}	-130.0^{-5}	-200.9^{-5}	12.35^{-3}	-4.45^{-1}		-5.23^{-2}
77	7	160	1.142	-8.58^{-1}	3.51^{-2}	128.4^{-5}	215.1^{-5}	12.20^{-3}	4.62^{-1}	1.64	1.32^{-2}
		160	1.142	-8.58^{-1}	3.51^{-2}	127.7^{-5}	210.6^{-5}	12.20^{-3}	4.55^{-1}		2.14^{-2}
78	7	150	1.140	-8.60^{-1}	4.29^{-2}	131.8^{-5}	221.9^{-5}	11.16^{-3}	4.76^{-1}	1.50	1.96^{-2}
		150	1.140	-8.60^{-1}	4.29^{-2}	129.8^{-5}	291.3^{-5}	11.16^{-3}	4.70^{-1}		1.95^{-2}
79	7	210	1.140	-8.60^{-1}	-4.29^{-2}	-131.4^{-5}	-226.5^{-5}	11.31^{-3}	-4.82^{-1}	1.52	-9.49^{-3}
		210	1.140	-8.60^{-1}	-4.29^{-2}	-131.1^{-5}	-224.5^{-5}	11.31^{-3}	-4.79^{-1}		-1.32^{-2}
80	6	219°5'	1.142	-8.58^{-1}	*	-109.9^{-5}	-199.9^{-5}	10.47^{-3}	-4.17^{-1}	1.41	*
		219°5'	1.142	-8.58^{-1}	*	-109.2^{-5}	-197.0^{-5}	10.47^{-3}	-4.12^{-1}		*
81	6	140°55'	1.142	-8.58^{-1}	*	112.2^{-5}	198.3^{-5}	10.71^{-3}	4.18^{-1}	1.44	*
		140°55'	1.142	-8.58^{-1}	*	111.9^{-5}	197.6^{-5}	10.71^{-3}	4.17^{-1}		*
82	6	170°32'	1.144	-8.56^{-1}	*	78.86^{-5}	120.2^{-5}	13.19^{-3}	2.68^{-1}	1.78	*
		170°32'	1.144	-8.56^{-1}	*	78.86^{-5}	120.9^{-5}	13.19^{-3}	2.69^{-1}		*
83	6	189°28'	1.144	-8.56^{-1}	*	-80.54^{-5}	-116.3^{-5}	13.44^{-3}	-2.65^{-1}	1.81	*
		189°28'	1.144	-8.56^{-1}	*	-78.86^{-5}	-113.4^{-5}	13.44^{-3}	-2.59^{-1}		*
84	8	192°3'	1.144	-8.56^{-1}	-2.37^{-2}	16.18^{-5}	-29.81^{-5}	10.67^{-3}	-1.83^{-2}	1.44	5.04^{-2}
			1.144	-8.56^{-1}	-2.37^{-2}	15.84^{-5}	-29.16^{-5}	10.67^{-3}	-1.79^{-2}		4.79^{-2}
85	8	167°57'	1.144	-8.56^{-1}	2.37^{-2}	-18.54^{-5}	29.81^{-5}	10.81^{-3}	1.52^{-2}	1.46	-5.68^{-2}
			1.144	-8.56^{-1}	2.37^{-2}	-18.54^{-5}	29.81^{-5}	10.81^{-3}	1.52^{-2}		-5.88^{-2}
86	8	140°23'	1.142	-8.58^{-1}	4.15^{-2}	-43.14^{-5}	35.96^{-5}	9.672^{-3}	-9.65^{-3}	1.30	-1.08^{-1}
			1.142	-8.58^{-1}	4.15^{-2}	-43.47^{-5}	35.32^{-5}	9.672^{-3}	-1.10^{-2}		-1.07^{-1}
87	8	219°37'	1.142	-8.58^{-1}	-4.15^{-2}	39.43^{-5}	-35.64^{-5}	9.721^{-3}	5.10^{-3}	1.31	9.49^{-2}
			1.142	-8.58^{-1}	-4.15^{-2}	40.44^{-5}	-36.61^{-5}	9.721^{-3}	5.15^{-3}		1.00^{-1}
88	9	200°10'	1.142	-8.58^{-1}	-3.28^{-2}	20.56^{-5}	-40.82^{-5}	10.47^{-3}	-2.73^{-2}	1.41	6.50^{-2}
			1.142	-8.58^{-1}	-3.28^{-2}	21.23^{-5}	-38.89^{-5}	10.47^{-3}	-2.38^{-2}		6.26^{-2}
89	9	159°50'	1.142	-8.58^{-1}	3.28^{-2}	-28.98^{-5}	44.71^{-5}	10.17^{-3}	2.12^{-2}	1.37	-1.03^{-1}
			1.142	-8.58^{-1}	3.28^{-2}	-29.66^{-5}	45.36^{-5}	10.17^{-3}	2.11^{-2}		-1.06^{-1}
			1.142	-8.58^{-1}	3.28^{-2}	-29.32^{-5}	43.74^{-5}	10.17^{-3}	1.94^{-2}		-1.01^{-1}
			1.142	-8.58^{-1}	3.28^{-2}	-29.32^{-5}	44.39^{-5}	10.17^{-3}	2.03^{-2}		-1.03^{-1}
91	9	209°47'	1.140	-8.60^{-1}	-3.26^{-2}	24.26^{-5}	-43.09^{-5}	9.721^{-3}	-2.52^{-2}	1.31	8.89^{-2}
			1.140	-8.60^{-1}	-3.26^{-2}	26.29^{-5}	-43.74^{-5}	9.721^{-3}	-2.35^{-2}		9.66^{-2}

Run 44 was repeat of run 43
Run 90 with Model 9 at 150°13' lost because of balance being out of alignment.

*Unable to measure moment arm A_3

UNCLASSIFIED

Security Classification

DOCUMENT CONTROL DATA - R&D

(Security classification of title, body of abstract and indexing annotation must be entered when the overall report is classified)

1. ORIGINATING ACTIVITY *(Corporate author)*
Arnold Engineering Development Center
ARO, Inc., Operating Contractor
Arnold Air Force Station, Tennessee

2a. REPORT SECURITY CLASSIFICATION
UNCLASSIFIED

2b. GROUP
N/A

3. REPORT TITLE
LIFT, DRAG, AND STATIC STABILITY OF A BLUNT CONICAL MODEL IN HYPERSONIC RAREFIED FLOW

4. DESCRIPTIVE NOTES *(Type of report and inclusive dates)*
N/A

5. AUTHOR(S) *(Last name, first name, initial)*
Boylan, David E., ARO, Inc.

6. REPORT DATE	7a. TOTAL NO. OF PAGES	7b. NO. OF REFS
March 1965	30	10

8a. CONTRACT OR GRANT NO.	9a. ORIGINATOR'S REPORT NUMBER(S)
AF 40(600)-1000	
b. PROJECT NO. 8953	AEDC-TR-65-62
c. Program Element 62405334	9b. OTHER REPORT NO(S) *(Any other numbers that may be assigned this report)*
d.	N/A

10. AVAILABILITY/LIMITATION NOTICES
Qualified requesters may obtain copies of this report from DDC.

11. SUPPLEMENTARY NOTES	12. SPONSORING MILITARY ACTIVITY
N/A	Arnold Engineering Development Center Air Force Systems Command Arnold AF Station, Tennessee

13. ABSTRACT

This is a report of results and analysis of measurements of forces on spherically capped cones of 10-deg half-angle, with and without conical afterbodies. These data were obtained during the course of an evaluation of a new three-component balance for use in a low-density, hypersonic wind tunnel. Comparisons are made with modified Newtonian and free-molecule theories. Measurements were made in nitrogen gas at a nominal Mach number of 9.8 and unit Reynolds number of 760 in.$^{-1}$. The suitability of the low-load, three-component balance for measuring aerodynamic forces in low-density flows is demonstrated.

DD FORM 1 JAN 64 1473

UNCLASSIFIED

Security Classification

14. KEY WORDS	LINK A		LINK B		LINK C	
	ROLE	WT	ROLE	WT	ROLE	WT
cones balance three-component hypersonic flow lift drag static stability aerodynamic forces measurement						

INSTRUCTIONS

1. ORIGINATING ACTIVITY: Enter the name and address of the contractor, subcontractor, grantee, Department of Defense activity or other organization *(corporate author)* issuing the report.

2*a*. REPORT SECURITY CLASSIFICATION: Enter the overall security classification of the report. Indicate whether "Restricted Data" is included. Marking is to be in accordance with appropriate security regulations.

2*b*. GROUP: Automatic downgrading is specified in DoD Directive 5200.10 and Armed Forces Industrial Manual. Enter the group number. Also, when applicable, show that optional markings have been used for Group 3 and Group 4 as authorized.

3. REPORT TITLE: Enter the complete report title in all capital letters. Titles in all cases should be unclassified. If a meaningful title cannot be selected without classification, show title classification in all capitals in parenthesis immediately following the title.

4. DESCRIPTIVE NOTES: If appropriate, enter the type of report, e.g., interim, progress, summary, annual, or final. Give the inclusive dates when a specific reporting period is covered.

5. AUTHOR(S): Enter the name(s) of author(s) as shown on or in the report. Enter last name, first name, middle initial. If military, show rank and branch of service. The name of the principal author is an absolute minimum requirement.

6. REPORT DATE: Enter the date of the report as day, month, year; or month, year. If more than one date appeara on the report, use date of publication.

7*a*. TOTAL NUMBER OF PAGES: The total page count should follow normal pagination procedures, i.e., enter the number of pages containing information.

7*b*. NUMBER OF REFERENCES: Enter the total number of references cited in the report.

8*a*. CONTRACT OR GRANT NUMBER: If appropriate, enter the applicable number of the contract or grant under which the report was written.

8*b*, 8*c*, & 8*d*. PROJECT NUMBER: Enter the appropriate military department identification, such as project number, subproject number, system numbers, task number, etc.

9*a*. ORIGINATOR'S REPORT NUMBER(S): Enter the official report number by which the document will be identified and controlled by the originating activity. This number must be unique to this report.

9*b*. OTHER REPORT NUMBER(S): If the report has been assigned any other report numbers *(either by the originator or by the sponsor)*, also enter this number(s).

10. AVAILABILITY/LIMITATION NOTICES: Enter any limitations on further dissemination of the report, other than those imposed by security classification, using **standard** statements such as:

(1) "Qualified requesters may obtain copies of this report from DDC."

(2) "Foreign announcement and dissemination of this report by DDC is not authorized."

(3) "U. S. Government agencies may obtain copies of this report directly from DDC. Other qualified DDC users shall request through _____."

(4) "U. S. military agencies may obtain copies of this report directly from DDC. Other qualified users shall request through _____."

(5) "All distribution of this report is controlled. Qualified DDC users shall request through _____."

If the report has been furnished to the Office of Technical Services, Department of Commerce, for sale to the public, indicate this fact and enter the price, if known.

11. SUPPLEMENTARY NOTES: Use for additional explanatory notes.

12. SPONSORING MILITARY ACTIVITY: Enter the name of the departmental project office or laboratory sponsoring *(paying for)* the research and development. Include address.

13. ABSTRACT: Enter an abstract giving a brief and factual summary of the document indicative of the report, even though it may also appear elsewhere in the body of the technical report. If additional space is required, a continuation sheet shall be attached.

It is highly desirable that the abstract of classified reports be unclassified. Each paragraph of the abstract shall end with an indication of the military security classification of the information in the paragraph, represented as *(TS)*, *(S)*, *(C)*, *or (U)*.

There is no limitation on the length of the abstract. However, the suggested length is from 150 to 225 words.

14. KEY WORDS: Key words are technically meaningful terms or short phrases that characterize a report and may be used as index entries for cataloging the report. Key words must be selected so that no security classification is required. Identifiers, such as equipment model designation, trade name, military project code name, geographic location, may be used as key words but will be followed by an indication of technical context. The assignment of links, rules, and weights is optional.